ENHANCED PRECIPITATION HARDENING IN Al-Mg(-Ag) ALLOYS

M. KUBOTA, J.F. NIE and B.C. MUDDLE

Department of Materials Engineering, Monash University, Clayton, Victoria, 3168, Australia

ABSTRACT The effects of microalloying additions of Ag (0.5 wt%) on the precipitation hardening response of an Al-10Mg (wt%) alloy, aged in the temperature range 160-240°C, have been examined using hardness measurements, transmission electron microscopy and electron diffraction. The Ag promotes an acceleration in the kinetics of the hardening response during isothermal ageing and a significant increase in the maximum hardness achievable. This enhancement of the hardening response is the result of changes in both the precipitation sequence and the identity of the primary strengthening precipitate phase(s). The work includes perhaps the first confirmed observation that the addition of Ag to Al-10Mg alloy leads to uniform precipitation of particles of an intermediate, metastable quasicrystalline phase during conventional isothermal ageing heat treatments.

Keywords: *precipitation hardening, Al-Mg(-Ag) alloys, Ag additions, high strength Al alloys, icosahedral phase*

1. INTRODUCTION

Alloys of the Al-Mg system have been a recent focus of attention for applications in the automobile and aerospace industries, because they possess a combination of high specific strength, relatively good formability, excellent resistance to corrosion and good weldability [1]. Commercial 5xxx series Al-Mg alloys are traditionally recognised as non-heat treatable alloys, because little or no precipitation hardening response is observed [2]. Increases in strength, based on precipitation hardening, may be achieved with an increase in Mg content. However, the strength increment is generally not regarded as sufficient to compensate for corresponding decreases in stress corrosion cracking resistance and hot workability [3].

It is well established that minor additions (~0.1 at%) of Ag to all Al alloys containing Mg enhance the precipitation hardening response, with an acceleration in precipitation kinetics and an increase in the maximum hardness achievable [4]. However, little attention has been paid to the effects of trace additions of Ag on binary Al-Mg alloys, with compositions within and beyond the current commercial range. Alloys of the Al-Mg system would appear to have strong potential for precipitation hardening, as it is easy to achieve supersaturated solid solutions with high concentrations of solute Mg [5]. However, alloys with <7-10 wt% Mg show little hardening and the hardness increment achievable at higher Mg contents is small. It is thus of interest to explore whether microalloying additions might be used to stimulate the precipitation hardening response.

Preliminary work has indicated that trace additions of Ag to binary Al-Mg alloys may improve the precipitation hardening response [6,7]. It was initially thought that the effect of Ag was to refine the distribution of the existing equilibrium precipitate phase [6]. However, Wheeler *et al.* [8] proposed that peak hardness in the ternary alloys is associated with fine-scale precipitates of a T phase, $Mg_{32}(Al,Ag)_{49}$ (b.c.c., space group $Im\bar{3}$, a = 1.416 nm) [9], rather than the equilibrium β, Al_3Mg_2 (f.c.c., space group $Fd\bar{3}m$, a = 2.824 nm) [10]. Auld and Cousland [11] analysed the ageing behaviour of a ternary Al-Mg-Ag alloy using X-ray diffraction techniques and revealed that the T phase thought to be present at peak hardness was, in fact, a metastable T' phase (h.c.p., a = 1.4 nm, c = 2.8 nm). Ito *et al.* [12] found that the solubility of magnesium in aluminium was decreased by the addition of 0.5wt% Ag, and concluded that the improvement in the age-hardening response was partly associated with an increased level of solute supersaturation at the ageing temperature. Takahashi *et al.* [13] examined the ageing behaviour of Al-10 wt% Mg alloys, with and without the addition of 0.5wt% Ag, and concluded that the increase in hardness of the ternary alloy was due to a fine-scale, homogeneous distribution of intermediate phases. However, as with previous studies, the precipitate microstructures were not well characterised and the role of Ag was not elucidated.

In the present study, the effects of Ag additions on the precipitation hardening response of an Al-10Mg (wt%) alloy, aged in the temperature range 160-240°C have been examined by measuring hardness, and the resulting precipitate microstructures characterised in detail using analytical transmission electron microscopy (TEM) and electron diffraction.

2. EXPERIMENTAL PROCEDURES

Experimental alloys with nominal compositions of Al-10Mg and Al-10Mg-0.5Ag (wt%) were prepared by induction melting and chill casting in air. The ingots were homogenised 72 h at 450°C, scalped and rolled to plates ~50 mm in thickness for hardness measurements, and to strips ~3 mm in thickness for TEM. All specimens were solution treated 1 h at 500°C in a salt bath, water quenched, and aged in oil baths for various times at temperatures in the range 160-240°C.

Bulk Vickers hardness was measured using a 5kg load; each measurement recorded is the result of at least 7 indentations. Discs 3 mm in diameter were punched from the aged strips, ground to a thickness of ~0.1 mm, and TEM thin foils were obtained by twin-jet electropolishing in a solution of 33% nitric acid and 67% methanol, at ~-10°C, 0.2A and ~12V. Specimens were examined in Philips EM420 and CM20 transmission electron microscopes operating at 120kV and 200kV respectively.

3. RESULTS AND DISCUSSION

3.1 Precipitation hardening response

The isothermal hardening response for the Al-10Mg and Al-10Mg-0.5Ag alloys, aged at 160, 200 and 240°C, are shown in Figures 1(a) and (b) respectively. The hardness of the binary alloy, Fig. 1(a), increases gradually from ~90 VHN in the as-quenched condition to maximum values of ~120, 110 and 105 VHN when aged at 160 (140 h), 200 (16 h) and 240°C (5 h) respectively. In the presence of Ag additions, Fig. 1(b), the hardening response is increased significantly, with values of maximum hardness of ~150, 140 and 120 VHN achieved at 160 (65 h), 200 (10 h) and 240°C (2 h), respectively. To place the observed hardness values in the Ag-modified alloys in perspective, it is worth noting that the maximum hardness of 140-150 VHN is comparable with that achievable in, for example, high strength Al-Cu-Mg-Ag alloys developed for aerospace applications [14,15]. The Al-Mg-Ag alloy holds a significant advantage in density.

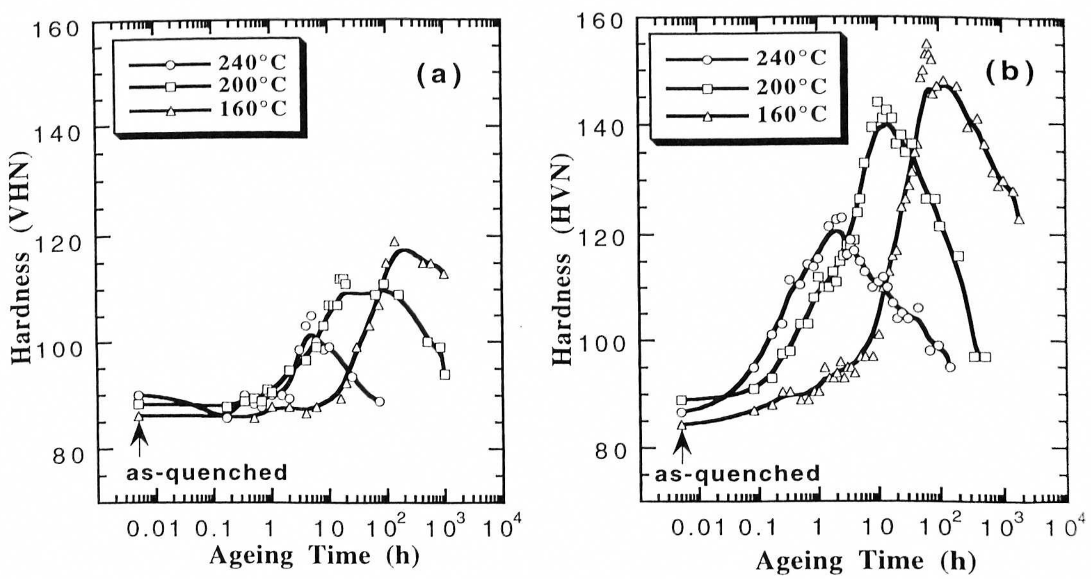

Fig. 1 Isothermal precipitation hardening response for (a) Al-10Mg, and (b) Al-10Mg-0.5Ag.

It is well-established that binary Al-Mg alloys with <5wt% Mg exhibit little or no age-hardening response and that it requires >7wt% Mg before a meaningful precipitation hardening becomes detectable [4]. For a given Mg content, the effect of Ag additions is both to accelerate the kinetics of the hardening response and to increase the maximum hardness achievable compared to binary alloy. The present results are consistent with those presented previously [13]. One potential source of this improved hardening response in the ternary alloys derives from observations [12] that as little as 0.5wt% Ag reduces the solubility of Mg in Al over the full range of temperatures below the eutectic temperature. Increased levels of solute supersaturation during ageing will not only increase the volume fraction of precipitate phase(s), but may also promote an increased nucleation rate leading to a finer and more uniform precipitate distribution. However, there is also evidence [8] that the Ag may promote a change in precipitate identity.

3.2 Microstructural characterisation in Al-10Mg(-0.5Ag) alloys aged at 240°C

Figures 2 (a) and (b) compare bright-field (BF) TEM micrographs of Al-10Mg and Al-10Mg-0.5Ag samples aged 0.5 h at 240°C. The electron beam is in each case approximately parallel to $<110>_\alpha$. In the under-aged Ag-free alloy, the microstructure contains coarse-scale, sparsely-dispersed lath-like precipitate particles, identified by electron diffraction to be β' phase (Al_3Mg_2, h.c.p., a = 10.02 nm, c = 16.36 nm) [2], Fig. 2(a). A dense distribution of dislocations surrounds the particles, suggesting that significant plastic accommodation accompanies nucleation and growth. In contrast, in the Ag-containing alloy, there is a distribution of fine-scale, faceted particles in the early stages of ageing, Fig. 2(b). Although becoming coarser approaching grain boundary precipitate-free zones, the otherwise uniform distribution of these fine particles is consistent with the higher hardness of the ternary alloy.

Figures 3(a)-(c) show a series of microbeam electron diffraction patterns recorded from one of the larger faceted particles in Fig. 2(b). The precipitate pattern recorded in Fig. 3(a) exhibits five-fold rotational symmetry, approximately parallel to a $<110>_\alpha$ orientation, while Fig. 3(b) reveals three-fold rotational symmetry in the precipitate diffraction pattern in this $<111>_\alpha$ orientation. There is two-fold symmetry in the precipitate pattern observed parallel to the $<112>_\alpha$ orientation in Fig. 3(c). These precipitate patterns are similar to those recorded from icosahedral phases in rapidly-quenched alloys [16]. Using models developed [17] for cubic approximants of icosahedral quasicrystals in the Al-Mg-Ag system, and a series of systematic large-angle tilting experiments, these patterns have been used to confirm [16,18] that these particles comprise a metastable, quasicrystalline phase that is a precursor to the T phase, $Mg_{32}(Al,Ag)_{49}$. It is to be emphasised that this metastable phase forms during conventional isothermal ageing and the present observations are perhaps the first in which a quasicrystalline phase has been shown to form as an intragranular solid state precipitate during conventional heat treatment.

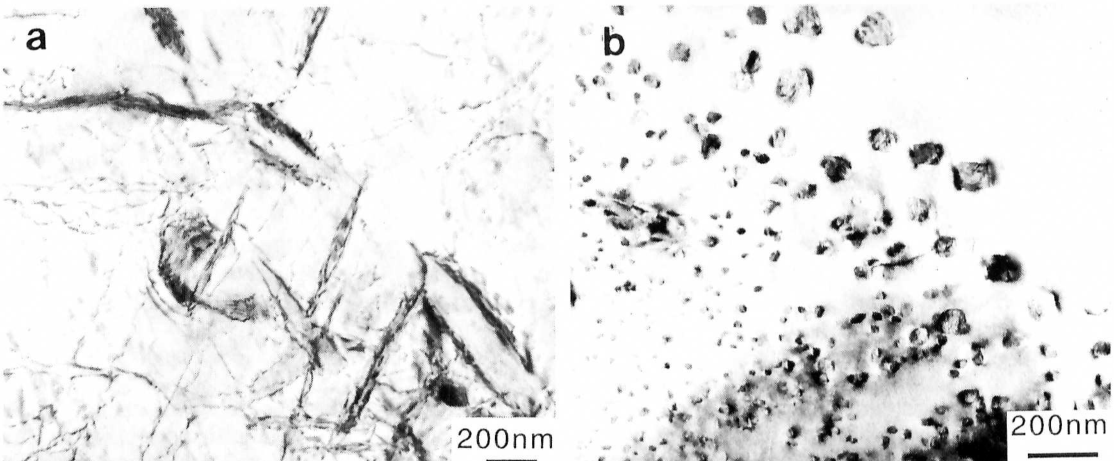

Fig. 2 TEM micrographs showing (a) Al-10Mg and (b) Al-10Mg-0.5Ag alloys aged 0.5 h at 240°C. The electron beam is approximately parallel to $<110>_\alpha$.

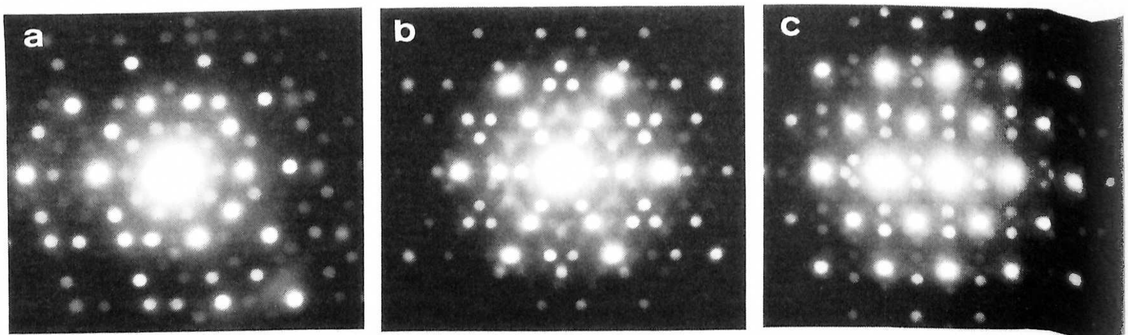

Fig. 3 Electron microdiffraction patterns recorded from a faceted particle such as in Fig. 2(b). Precipitate patterns show (a) 5-fold, (b) 3-fold and (c) 2-fold rotational symmetries parallel to $\langle 110\rangle_\alpha$, $\langle 111\rangle_\alpha$ and $\langle 112\rangle_\alpha$ respectively.

Figures 4 (a) and (b) compare BF TEM micrographs of Ag-free and Ag-containing alloys respectively, each sample aged to maximum hardness at 240°C. The electron beam is in each case approximately parallel to $\langle 001\rangle_\alpha$. The microstructure in the binary alloy, Fig. 4(a), contains a coarse distribution of metastable β' precipitate laths, together with an array of irregularly-shaped, randomly-oriented particles identified as the equilibrium β phase [10]. However, compared to the binary alloy, the scale and morphology of the precipitate particles are refined by the trace additions of Ag. There is a uniform, fine-scale distribution of rod-like particles in the Al-Mg-Ag alloy at maximum hardness, Fig. 4(b).

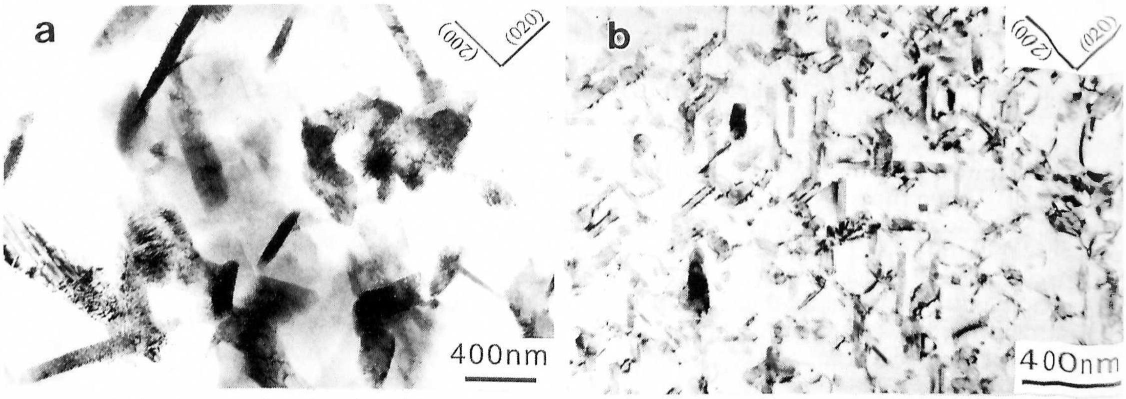

Fig. 4 TEM micrographs showing (a) Al-10Mg alloy aged 5 h, and (b) Al-10Mg-0.5Ag alloy aged 1 h, at 240°C. Electron beam is approximately parallel to $\langle 001\rangle_\alpha$.

Figures 5(a), (b) and (c) present electron microdiffraction patterns recorded from the rod-like particles in the Ag-modified alloy parallel to $\langle 1\bar{1}0\rangle_\alpha$, $\langle 112\rangle_\alpha$ and $\langle 11\bar{1}\rangle_\alpha$ directions respectively. As shown in the accompanying schematic solutions, these patterns can be indexed for the T phase [9]. The orientation relationship between the T phase and the matrix is of the form: $(010)_T \parallel (11\bar{1})_\alpha$ and $[001]_T \parallel [1\bar{1}0]_\alpha$. There are two distinguishable sets of orthogonal, elongated precipitate particles in Fig. 4(b). One set has traces parallel to $\langle 110\rangle_\alpha$ directions; in the other set, the particles are elongated parallel to $\langle 100\rangle_\alpha$ directions. The distribution is consistent with a single array of rod-like forms, with rod axes parallel to $\langle 110\rangle_\alpha$ directions.

The T phase has been interpreted to be the equilibrium phase in aged Al-Mg-Ag alloys [19]. However, the present characterisation has revealed that the rod-like T phase is metastable and replaced by equilibrium β phase in overaged samples. The β phase forms in a bi-modal distribution of coarse globular particles and smaller spheroidal particles in samples aged at 240°C, Fig. 6(a). The orientation relationship between the β phase and matrix α-Al phase is of the form $(100)_\beta \parallel (100)_\alpha$ and $[001]_\beta \parallel [001]_\alpha$, which is a relationship distinguishable from that previously reported [20]. The coarse, globular particles commonly contain a substructure involving multiple twinning, Fig. 6(b).

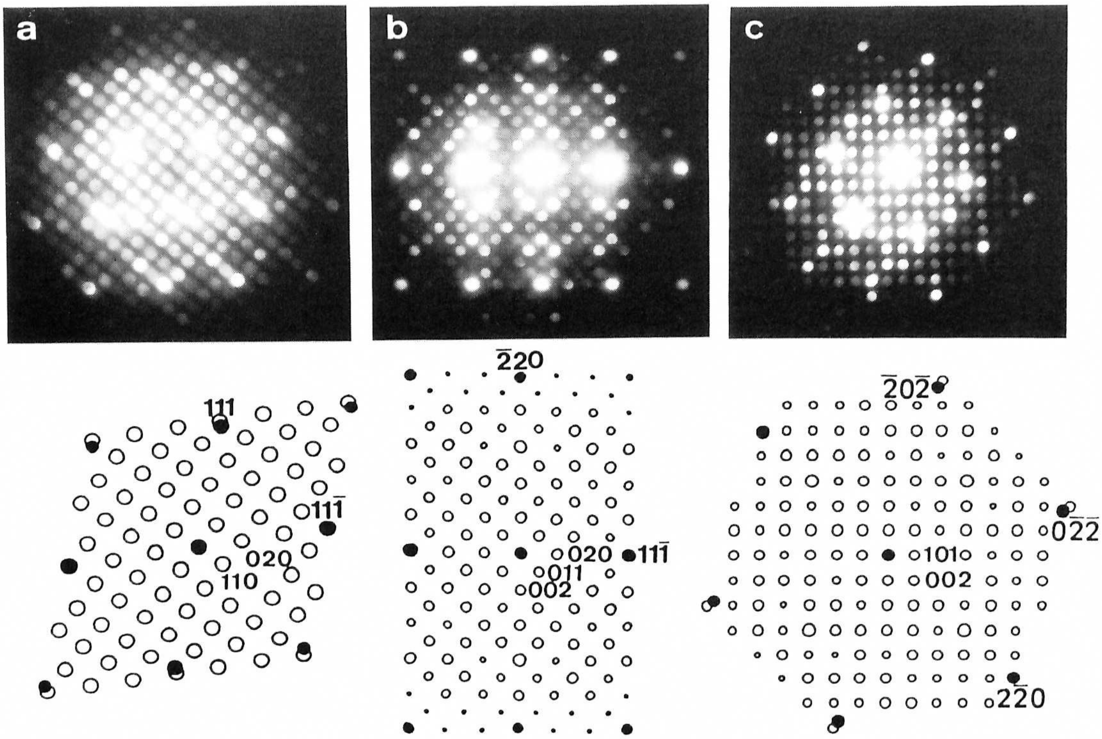

Fig. 5 Electron microdiffraction patterns recorded from single rod-like particle in Al-10Mg-0.5Ag alloy, with th beam parallel to (a) $\langle 1\bar{1}0\rangle_{\alpha}$, (b) $\langle 112\rangle_{\alpha}$ and (c) $\langle 11\bar{1}\rangle_{\alpha}$. The computed patterns are indexed for the (a) $\langle 001\rangle_{T}$, (b) $\langle\bar{1}00\rangle_{T}$ and (c) $\langle 010\rangle_{T}$ zone axes.

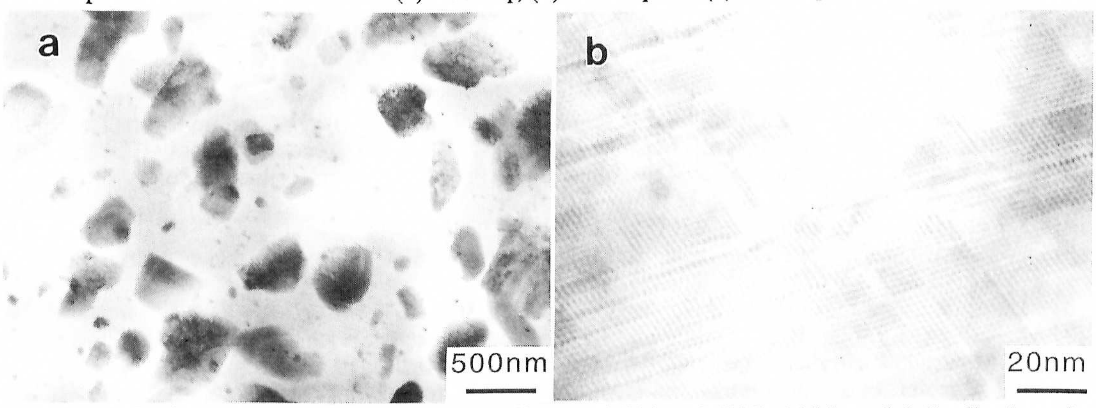

Fig. 6 TEM micrographs of Al-10Mg-0.5Ag alloy aged 72 h at 240°C; (a) bi-modal distribution of equilibrium β phase, and (b) substructure of β phase particle.

3.3 Microstructural characterisation in Al-10Mg(-0.5Ag) alloys aged at 160°C

Microstructural characterisation of binary Al-10Mg alloy in the under-aged condition at 160°C revealed two types of precipitates; one sparsely-distributed in cuboidal form, identified as equilibrium β phase, and the other, plate-like metastable β' particles, with a habit plane of $\{100\}_{\alpha}$. In contrast, microstructure of the Ag-modified alloy contained uniformly distributed fine particles, together with a few sparsely-distributed plate-like particles. Identification of the smaller particles in the early stages of ageing proved difficult because of their small scale. However, SAED patterns from areas dense in these particles indicated that they were similar to the icosahedral phase in the under-aged, Ag-modified specimens aged at 240°C. The scale of the particles in the sample aged at 160°C was much smaller than those in samples aged at 240°C, and there was a lower volume fraction of the $\langle 001 \rangle_\alpha$ plate-like particles, which were identified as metastable β' phase.

SUMMARY

(1) The precipitation hardening response of binary Al-10Mg alloy may be significantly enhanced by microalloying additions of Ag. The presence of Ag accelerates the kinetics of ageing and stimulates a precipitation sequence that contributes a substantial increase in precipitation hardening.

(2) The enhanced precipitation hardening attributable to microalloying with Ag is the result of changes in both the precipitation sequence and the identity of the strengthening precipitates. Phases stimulated by the addition of Ag are refined and more densely distributed than those in Al-10Mg.

(3) Microstructural observations combined with microbeam electron diffraction analysis suggest the following precipitation sequences in Al-10Mg(-0.5Ag) (wt%) alloys aged isothermally at:

(i) 160°C

Al-10Mg: α ----> metastable β' (h.c.p.) ----> equilibrium β (f.c.c.)
Al-10Mg-0.5Ag: α ----> metastable icosahedral (T) phase + metastable β' (h.c.p.) ----> metastable crystalline T phase (b.c.c.) ----> equilibrium β (f.c.c.)

(ii) 240°C

Al-10Mg: α ----> metastable β' phase (h.c.p.) ----> equilibrium β (f.c.c.)
Al-10Mg-0.5Ag: α----> metastable icosahedral (T) phase ----> metastable crystalline T phase (b.c.c.) ----> equilibrium β (f.c.c.)

(4) The present observations are perhaps the first to reveal that the addition of Ag to Al-10Mg alloy stimulates a metastable quasicrystalline form of the T phase during conventional isothermal ageing treatments. This phase is a precursor to crystalline T phase, which is the metastable intermediate phase primarily responsible for maximum hardness in Ag-modified alloys.

ACKNOWLEDGEMENTS

The authors acknowledge gratefully support from the Australian Research Council and assistance from Emeritus Professor I.J. Polmear. One author (MK) also acknowledges receipt of a Monash Graduate Scholarship and an Overseas Postgraduate Research Award.

REFERENCES

[1] R.E. Sanders, Jr., S.F. Baumann and H.C. Stumpf: Aluminum Alloys-Contemporary Research and Applications, Edited by A.K. Vasudevan and R.D. Doherty, Academic Press (1989), 85.
[2] L.F. Mondolfo: Aluminum Alloys, Structure and Properties, Butterworths,London (1976), 311.
[3] A.T. Thomas: J. Inst. Metals, 94 (1966), 37.
[4] I.J. Polmear: Trans. Met. Soc. AIME, 230 (1964), 1331.
[5] G.W. Lorimer: Precipitation Process in Solids, Edited by K.C. Russell and H.I. Aaronson, T.M.S-A.I.M.E., Warrendale Pennsylvania (1978), 97.
[6] I.J. Polmear and K.R. Sargant: Nature, 200 (1963), 669.
[7] M. Kubota, J.F. Nie, B.C. Muddle and I.J. Polmear: Proc. Mat. Res. '96, Vol. 1, Inst. Metals and Materials Australasia (IMMA), Brisbane, Australia (1996), 17.
[8] M.J. Wheeler, G. Blankenburgs and R.W. Staddon: Nature, 207 (1965), 746.
[9] G. Bergman, J.L.T. Waugh and L. Pauling: Acta. Cryst., 10 (1957), 254.
[10] A. Samson: Acta Cryst., 19 (1965), 401.
[11] J.H. Auld and S. McK. Cousland: Metal Science, 10 (1976), 445.
[12] T. Ito, T. Furuya, K. Matsuura and K.Watanabe: J. Jpn. Inst. Metals, 33 (1969), 1232; Trans., JIM, 12 (1971), 379.
[13] T.Takahashi, Y. Kojima and S. Okaniwa: J. Jpn. Inst. Metals, 42 (1978), 396.
[14] J.A. Taylor, B.A. Parker and I.J. Polmear: Metal Science, 12 (1978), 478.
[15] I.J. Polmear and M.J. Couper: Metall. Trans. A, 19A (1988), 1027.
[16] D. Shechtman, I. Blech, D. Gratias and J.W. Cahn: Phys. Rev. Lett., 53 (1984), 1951.
[17] G. Kreiner and S. Spiekermann: J. Alloys and Compounds, 261 (1997), 62.
[18] M. Kubota, J.F. Nie and B.C. Muddle: Phil. Mag. A, to be submitted (1998).
[19] B.E. Williams: J. Aust. Inst. Met., 17 (1972), 171.
[20] M. Bernole, J. Raynal and R. Graf: J. Microscopie, 8 (1969), 831.